Ubiquitin orchestrates proteasome dynamics between proliferation and quiescence in yeast

Zhu Chao Gu[a], Edwin Wu[a], Carolin Sailer[a,†], Julia Jando[a,‡], Erin Styles[b], Ina Eisenkolb[a,†], Maike Kuschel[a,†], Katharina Bitschar[a], Xiaorong Wang[c], Lan Huang[c], Adriano Vissa[b], Christopher M. Yip[a,b], Ravikiran S. Yedidi[a], Helena Friesen[b], and Cordula Enenkel[a,*]

[a]Department of Biochemistry, University of Toronto, Toronto, ON M5G 1M1, Canada; [b]Donnelly Centre, University of Toronto, Toronto, ON M5S 3E1, Canada; [c]Department of Physics and Biophysics, University of California, Irvine, Irvine, CA 92697

ABSTRACT **Proteasomes are essential for protein degradation in proliferating cells. Little is known about proteasome functions in quiescent cells. In nondividing yeast, a eukaryotic model of quiescence, proteasomes are depleted from the nucleus and accumulate in motile cytosolic granules termed proteasome storage granules (PSGs). PSGs enhance resistance to genotoxic stress and confer fitness during aging. Upon exit from quiescence PSGs dissolve, and proteasomes are rapidly delivered into the nucleus. To identify key players in PSG organization, we performed high-throughput imaging of green fluorescent protein (GFP)-labeled proteasomes in the yeast null-mutant collection. Mutants with reduced levels of ubiquitin are impaired in PSG formation. Colocalization studies of PSGs with proteins of the yeast GFP collection, mass spectrometry, and direct stochastic optical reconstitution microscopy of cross-linked PSGs revealed that PSGs are densely packed with proteasomes and contain ubiquitin but no polyubiquitin chains. Our results provide insight into proteasome dynamics between proliferating and quiescent yeast in response to cellular requirements for ubiquitin-dependent degradation.**

Monitoring Editor
Thomas Sommer
Max Delbrück Center for Molecular Medicine

Received: Mar 14, 2017
Revised: Jun 16, 2017
Accepted: Jul 24, 2017

INTRODUCTION

The proteasome is a 2.5-MDa, multisubunit protease complex responsible for the degradation of proteins conjugated to polyubiquitin chains. Failures in ubiquitin-proteasome-dependent protein degradation result in intracellular accumulations of irreversible and immotile ubiquitin-containing protein inclusions, which are indicative for age-related neurodegenerative diseases (Ciechanover and Brundin, 2003; Goldberg, 2003; Zheng *et al.*, 2016). However, not all protein inclusions detected in centenarians' brain tissues consist of irreversible and immotile proteins (Haller *et al.*, 2013; Xekardaki *et al.*, 2015). Protein inclusions that are reversible and motile, such as proteasome granules, may even protect from the early onset of neurodegenerative diseases (Amen and Kaganovich, 2015).

Proteasome granules have an enigmatic structure. The mechanism underlying their organization is unknown but seems to be conserved, as proteasome granules are found in nondividing quiescent yeast and human neuronal cells (Enenkel, 2014).

Quiescence is a reversible state in which cell proliferation is temporarily arrested during chronological aging (O'Farrell, 2011; Valcourt *et al.*, 2012). Drastic metabolic changes accompany the transition from proliferation to quiescence. The genome undergoes significant topological reorganizations (Rutledge *et al.*, 2015), and multiple molecules accumulate in storage compartments (Gray *et al.*, 2004; De Virgilio, 2012). Global repression of transcription and translation ensures longevity of the quiescent state (Miles *et al.*, 2013; McKnight *et al.*, 2015).

Proteasome granules are the result of proteasome reorganizations during quiescence, as thousands of individual proteasomes gather within one to two membrane-less organelles. In yeast, proteasome granules were originally named proteasome storage

This article was published online ahead of print in MBoC in Press (http://www.molbiolcell.org/cgi/doi/10.1091/mbc.E17-03-0162) on August 2, 2017.

*Address correspondence to: Cordula Enenkel (cordula.enenkel@utoronto.ca).

Present addresses: †Institute of Biochemistry, University of Stuttgart, Pfaffenwaldring 55, D-70569 Stuttgart, Germany; ‡Institute of Physiology, University of Zürich, CH-8057 Zürich, Switzerland.

Abbreviations used: CP, core particle; DAPI, 4′,6-diamidino-2-phenylindole; DIC, differential interference contrast; dSTORM, direct stochastic optical reconstitution microscopy; GFP, green fluorescent protein; GFPS, GFP–Strep-Tactin; IPOD, insoluble protein deposits; JUNQ, juxtanuclear quality compartments; LC-MS/MS, liquid chromatography–tandem mass spectroscopy; ORF, open reading frame; PSG, proteasome storage granule; RFP, red fluorescent protein; RP, regulatory particle; Rpn, regulatory particle non-ATPase; Rpt, regulatory particle triple-A (AAA) ATPase; TIRF, total internal reflection fluorescence; YPD, yeast peptone glucose.

© 2017 Gu *et al.* This article is distributed by The American Society for Cell Biology under license from the author(s). Two months after publication it is available to the public under an Attribution–Noncommercial–Share Alike 3.0 Unported Creative Commons License (http://creativecommons.org/licenses/by-nc-sa/3.0).

"ASCB®," "The American Society for Cell Biology®," and "Molecular Biology of the Cell®" are registered trademarks of The American Society for Cell Biology.

granules (PSGs), presumably protecting proteasomes from degradation (Laporte *et al.*, 2008). PSGs are primarily detected at a young replicative age. Their presence confers cell fitness during chronological aging (van Deventer *et al.*, 2015) and resilience toward geno- and proteotoxic stress (Ratnakumar *et al.*, 2011; Doherty *et al.*, 2012; Weberruss *et al.*, 2013; van Deventer *et al.*, 2015).

Proteasomes are the second most abundant protein complexes in eukaryotic cells (Marguerat *et al.*, 2012). Composed of ~40 different subunits, proteasome holo-enzymes consist of the proteolytic core particle (CP) flanked by one or two regulatory particles (RPs) (Baumeister *et al.*, 1998). The CP comprises two outer and two inner rings of seven distinct α and β subunits, respectively. The β-rings harbor the proteolytic sites. The α-rings control the access of protein substrates that are delivered by the RP. The RP is composed of approximately nine lid and approximately 10 base subunits, of which distinct Rpn (regulatory particle non-ATPase) subunits recognize the polyubiquitin chain. The ubiquitin moieties are cleaved before substrate degradation (Peth *et al.*, 2010; Rosenzweig *et al.*, 2012). The RP lid subunit Rpn11 catalyzes the en bloc removal of the polyubiquitin chain (Verma *et al.*, 2002; Yao and Cohen, 2002), while the proteasome-associated protein Ubp6, the yeast homologue of USP14, catalyzes the removal of supernumerary polyubiquitin chains (Lee *et al.*, 2016), thus allowing gradual deubiquitylation of the substrate (Crosas *et al.*, 2006; Hanna *et al.*, 2006). The deubiquitylated substrate is translocated into the proteolytic chamber of the CP through Rpt (regulatory particle triple-A (AAA) ATPase) subunits adjacent to the CP α-ring (Rabl *et al.*, 2008). During cell proliferation, when the intracellular ATP level is high (Laporte *et al.*, 2011), the RP is attached to the CP, yielding proteasome holo-enzymes that are primarily located in the nucleus and are functionally active for degrading polyubiquitinylated proteins (Tanaka, 2009; Enenkel, 2014).

In yeast, the ATP level declines with the transition from proliferation to quiescence due to glucose depletion in stationary phase (Laporte *et al.*, 2011). The intracellular pH drops, and the protoplasmic fluidity decrease impacts the dynamics of soluble proteins (Laporte *et al.*, 2011; Parry *et al.*, 2014; Munder *et al.*, 2016). Proteasomes accumulate at the inner side of the nuclear envelope (Laporte *et al.*, 2008), pass through the nuclear pore, and gather in an early intermediate of the PSG, which yields the mature PSGs separate from insoluble protein deposits (IPOD) (Kaganovich *et al.*, 2008; Peters *et al.*, 2016).

Although CP and RP colocalize within the PSGs, RP–CP assemblies are less stable in carbon- (Bajorek *et al.*, 2003; Orlowski and Wilk, 2000; Weberruss *et al.*, 2013) or nitrogen-starved cells (Waite *et al.*, 2016). The instantaneous gain of ATP that occurs upon glucose feeding of carbon-starved cells triggers the resumption of growth and the immediate clearance of PSGs. Within a few minutes, RP–CP assemblies are formed that relocate to the nucleus, illustrating the reversible and motile nature of the PSGs (Laporte *et al.*, 2008; Weberruss *et al.*, 2013).

A genome-wide systematic screen in proliferating yeast revealed that lowering the intracellular pH induces premature PSG formation (Peters *et al.*, 2013). It is conceivable that pH and metabolites influence proteasome assembly and intracellular movement, but the key proteins controlling proteasome dynamics and PSG organization remained unknown. Based on our previous studies, Blm10 is the only protein known to be involved in the sequestration of the CP into PSGs. Its absence affects the sequestration of the CP but not of the RP (Weberruss *et al.*, 2013).

PSGs, which share the feature of reversibility with juxtanuclear quality compartments (JUNQ) (Kaganovich *et al.*, 2008), are not the only spherical structures of proteasome sequestrations. Cell cycle arrest by proteasome inhibition or nitrogen starvation also induces the sequestration of proteasomes, although in irreversible and immotile protein inclusions that resemble IPOD-like structures (Marshall *et al.*, 2016). When either the proteasome is inactivated or essential amino acids are depleted, the proteasome becomes polyubiquitinylated and is sacrificed for Atg8-mediated autophagic degradation (Marshall *et al.*, 2015, 2016; Cohen-Kaplan *et al.*, 2016). Dysfunctional and misassembled proteasomal subunits are also sequestered into IPOD-like compartments for final degradation (Peters *et al.*, 2015). The lysosomal targeting of these proteasomal components appear to be specific for nitrogen starvation but is not observed under glucose starvation (Waite *et al.*, 2016).

Yeast cells were grown in yeast peptone glucose (YPD) media at 30°C throughout this work to avoid mixed phenotypes with reversible and irreversible proteasome granules due to limitations of carbon and nitrogen sources.

Applying high-throughput microscopy to the yeast null-mutant collection, we screened for genes required for the orchestrated sequestration of the CP and RP into the PSGs. We also screened the yeast collection of green fluorescent protein (GFP)-labeled open reading frames (ORFs) for proteins that form reversible and motile granules in quiescence. Both screens identified genes that are involved in balancing the load of polyubiquitin chains on the proteasome versus the concentration of free ubiquitin. Reduced levels of free ubiquitin were paralleled with impaired PSG formation. Using mass spectrometry and direct stochastic optical reconstitution microscopy (dSTORM) analysis, in vivo cross-linked PSGs were found to be densely packed and primarily composed of CP, RP, and free ubiquitin. Overexpression of lysine-less ubiquitin variants induced premature PSG formation during proliferation. On the basis of these findings, we propose a model for proteasome movements in proliferating and quiescent cells in response to cellular requirements for ubiquitin-dependent degradation.

RESULTS

Systematic identification of yeast null mutants with deficiencies in PSG formation

To shed light into proteasome dynamics in yeast, we set out to explore genes that are involved in the sequestration of proteasomes into PSGs by exploiting high-throughput imaging screens based on automated image acquisition coupled with the quantification of specific morphological phenotypes (Boone *et al.*, 2007; Tong *et al.*, 2001). To systematically survey the yeast deletion collection for defects in PSG formation, we created a library of ~4300 null mutants expressing the GFP-labeled variant of the β5-subunit Pre2 (Pre2-GFP), which is a well-established reporter protein of the CP (Figure 1A) (Enenkel, 2012). In addition to Pre2-GFP, mCherry-labeled histone Hta2 (Hta2-mCherry) and the ribosomal *RPL39* promoter region driving expression of tdTomato (RPL39pr-dtTomato) were crossed into the arrayed collection of null mutants as markers of the nucleus and cytoplasm, respectively (Supplemental Figure S1).

Forty-five null mutants were identified with deficiencies in PSG formation (Supplemental Table S1). The mutants were grouped according to their biological functions: 1) nuclear transport; 2) ubiquitin modifying proteins; 3) proteins regulating energy levels; 4) kinases and phosphatases; 5) DNA repair and chromatin remodeling; and 6) proteins with miscellaneous functions. V-type ATPases involved in premature PSG formation in proliferating cells (Peters *et al.*, 2013) were not among our hit genes, consistent with the finding that V-type ATPases disassemble with glucose deprivation in quiescence (Martinez-Munoz and Kane, 2008).

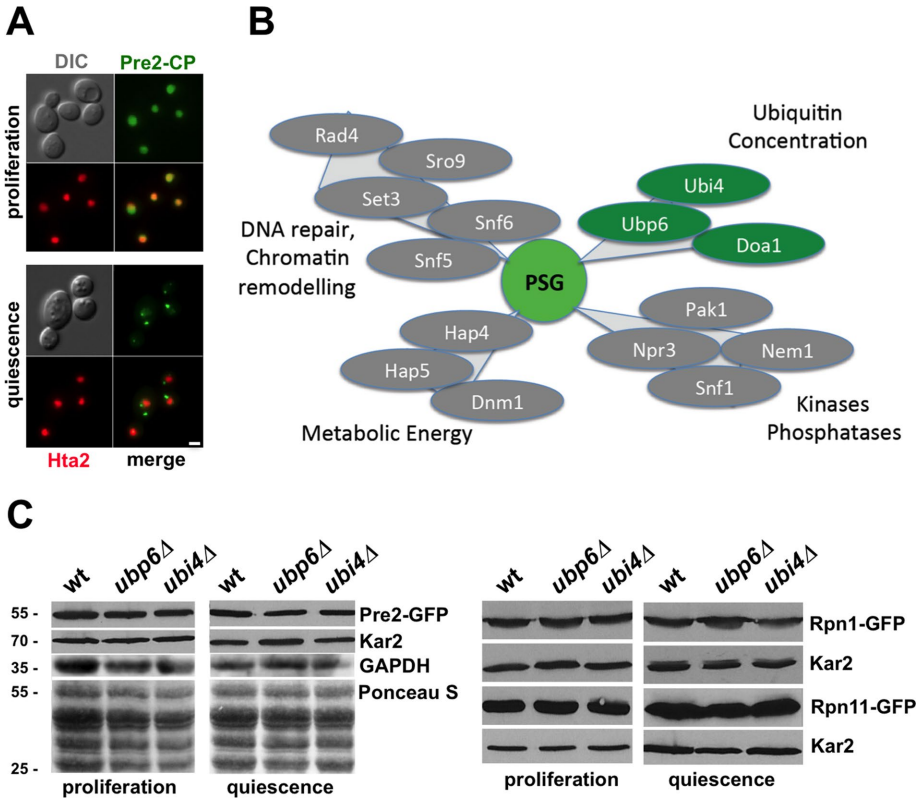

FIGURE 1: High-throughput survey for yeast null mutants with perturbed PSG formation. (A) Direct fluorescence microscopy of proteasome localization in the query wild-type (WT) cells expressing GFP-labeled CP subunit Pre2 (Pre2-GFP) and Hta2-mCherry. Cells were monitored during cell proliferation (corresponding to growth to logarithmic phase, OD_{600} ~ 1.0) or during quiescence (corresponding to stationary phase, OD_{600} ~ 10) by using differential interference contrast (DIC), GFP, and RFP filter sets. Scale bar: 3 µm. (B) Proteins required for orchestrating the sequestration of CP, RP lid, and RP base complexes into PSGs were assigned to functional groups as listed in Table 1. (C) Protein levels of GFP-labeled Pre2, RP base subunit Rpn1, and RP lid subunit Rpn11 in wild-type, *ubp6*Δ, and *ubi4*Δ cells were analyzed by SDS–PAGE and Western blotting using antibodies against GFP, Kar2, and GAPDH. Western blots were stained by Ponceau S before antibodies were added.

A high-throughput imaging screen of temperature-sensitive mutants of essential genes turned out to be hardly feasible, because each mutant requires a specific restrictive temperature and incubation time to display its phenotype in quiescence (e.g., *uba1-1* mutants of the ubiquitin-activating enzyme Uba1 [Shimada *et al.*, 2002] formed PSGs upon growth for 3 d at 35°C).

Because CP and RP colocalize within PSGs, our main focus was directed toward proteins that orchestrate the sequestration of the CP and RP into the PSGs. The hit mutants that were identified using Pre2-GFP were assayed with GFP-labeled RP base subunit Rpn1 and lid subunit Rpn11 (Rpn1-GFP, Rpn11-GFP). Once again, Hta2-mCherry and cytosolic RPL39pr-tdTomato marked the nucleo- and cytoplasm, respectively. Twenty-one null mutants showed perturbed sequestration of the RP into PSGs, suggesting that the sequestration of the CP and RP into PSGs depends on the same genes in these null mutants. The cutoff for marking a defect in these mutants was set to 30% PSG formation compared with the wild type (Table 1; 15 mutants could be grouped by related functions as shown in Figure 1B). None of the mutants fell into the category of mutants that fail to enter quiescence (Li *et al.*, 2015), consistent with our observation that disturbed PSG formation was not caused by blocked upstream processes such as nuclear retention of proteasomes.

Blm10 was identified in the high-throughput imaging analysis as a protein known to be involved in the sequestration of the CP into PSGs. Because *BLM10* deletion does not impair the sequestration of the RP into the PSGs (Weberruss *et al.*, 2013), Blm10 does not fulfill the criterion of a protein orchestrating PSG formation (see the Supplemental Material for *blm10*Δ strains with two different genetic backgrounds; Supplemental Figure S2).

As shown by our previous studies on *blm10*Δ mutants, the deficiency in PSG formation is linked with a delay in the resumption of growth upon exit from quiescence, notably after DNA damage by phleomycin (Weberruss *et al.*, 2013). To test the correlation between delayed outgrowth from quiescence and failures in PSG formation in our hit mutants, we plotted regrowth curves for lag-phase differences with and without phleomycin. Eight hit mutants showed delays in the resumption of growth upon exit from quiescence and perturbed PSG formation (Supplemental Figure S3A). Among them were null mutants of *UBP6*, *UBI4*, and *DOA1* involved in the regulation of the cellular ubiquitin concentration (Kraut *et al.*, 2007) (Supplemental Figure S3B). SDS–PAGE and Western blot analysis verified that each GFP-labeled proteasomal reporter subunit is expressed during proliferation and quiescence (Figure 1C, wild type, *ubp6*Δ, and *ubi4*Δ).

In particular, the deletion of *UBP6* and *UBI4* resulted in PSG frequencies below 10% (Figure 2A, wild type and *ubp6*Δ cells; Figure 2C, *ubi4*Δ cell; Figure 2, B and D, quantification). The null mutant of *DOA1* displayed ~30% PSG formation and was omitted from follow-up investigations. In the hit mutants, proteasomes were equally abundant, showing that disturbed PSG formation is not caused by proteasome depletion (Supplemental Figures S7 and S8).

UBP6 codes for a proteasome-associated ubiquitin-specific protease that contributes to the replenishment of ubiquitin (Crosas *et al.*, 2006; Sakata *et al.*, 2011). *UBI4* encodes a penta-repeat of ubiquitin molecules and is required to resist starvation and stress in stationary phase (Finley *et al.*, 1987). Both *ubp6*Δ and *ubi4*Δ mutants are characterized by low levels of free ubiquitin (Figure 2E) (Hanna *et al.*, 2006, 2007).

To test whether the perturbed PSG phenotype of *ubp6*Δ mutants is caused by the lack of the ubiquitin hydrolase activity of Ubp6, we analyzed the active-site mutant Ubp6-C118A (*ubp6*-C118A) for PSG formation. The *ubp6*Δ cells were transformed with centromere-based plasmids expressing either wild type or Ubp6-C118A. In addition, Pre2-, Rpn1-, and Rpn11-GFP were coexpressed to monitor the localization of the CP, RP base, and RP lid, respectively. Fluorescence microscopy revealed that PSGs are formed in reconstituted wild type but not in the *ubp6*-C118A active-site mutant (Figure 3A). Again, the ubiquitin level in the *ubp6*-C118A active-site mutant was confirmed to be lower than in wild type (Figure 2E).

Gene product	% CP	% RP base	% RP lid	Granule
Ubiquitin-modifying proteins				
Doa1	–	–	–	+
Ubi4	–	–	–	+ + +
Ubp6	–	–	–	+ + +
Regulators of energy levels				
Dnm1	–	–	–	+
Hap4	–	–	–	–
Hap5	–	–	–	–
Kinases and phosphatases				
Nem1	–	–	–	+
Npr3	–	–	–	n.d.
Pak1	+	–	+	+
Snf1	+	–	–	+
DNA repair, chromatin remodeling				
Rad4	+	–	–	–
Set3	–	–	–	+
Snf5	+	–	–	+
Snf6	+	–	+	+
Sro9	–	–	–	+
Proteins with miscellaneous functions				
Ade4	–	–	–	+
Cpr7	+	–	–	–
Icl1	–	–	–	n.d.
Sec66	–	–	+	–
Tps2	–	–	–	–
Vps24	+	–	–	+

Null mutants of selected hit genes expressing either Pre2-, Rpn1-, or Rpn11-GFP were manually analyzed for PSG formation in quiescence. Two hundred cells were monitored by direct fluorescence microscopy. The percentage of cells that sequester CP, RP lid, and RP base into the PSG was counted. –, less than 30%, + between 30% and 50% of the respective proteasomal complex is sequestered into the PSGs. The sequestration of the hit gene products into cytosolic granules in quiescence was analyzed by monitoring wild-type cells expressing GFP-labeled versions of the hit gene products, respectively. All protein granules formed by the respective GFP-labeled gene product were tested for reversibility upon exit from quiescence. Reversible and motile protein granules are designated in red (+), irreversible and immotile in black (+). Proteins colocalizing with PSGs were are designated (+ + +); n.d. the localization could not be detected.

TABLE 1: Proteins required for PSG formation identified in imaging screen with deletion collection.

We next analyzed whether proteasome relocalization into the nucleus is delayed in *upb6*Δ and *ubp6*-C118A mutants upon exit from quiescence, when PSGs resolve and mature proteasomes reappear within a few minutes in the nucleus of wild-type cells. In *upb6*Δ and *ubp6*-C118A mutants lacking PSGs, the replenishment of nuclear proteasomes took more than one regular generation time (Figure 3, B and D, top graph); *ubi4*Δ cells displayed similar phenotypes (Figure 3, C and D, bottom graph). Thus perturbed PSG formation is connected with the inability to rapidly relocate proteasomes into the nucleus upon growth resumption. Perturbed PSG formation may also contribute to the hypersensitivity of *upb6*Δ and *ubi4*Δ mutants toward a variety of agents inducing proteo- and genotoxic stress (Finley *et al.*, 1987; Chernova *et al.*, 2003).

PSGs are unique cytosolic granules densely packed with proteasomes

To extend our search for possible PSG scaffold proteins, we performed a systematic survey for proteins forming PSG-like structures by high-throughput imaging of the collection of strains expressing ~4100 GFP-labeled ORFs (Huh *et al.*, 2003). Hta2-mCherry was crossed into the arrayed strain collection as marker of the nucleus. The screen was performed by automated imaging analysis using the Evotec Opera microscope and analyzed manually by eye. Only when three individuals independently found matching results was a strain counted as a hit.

In follow-up experiments, each hit strain was manually analyzed for PSG-like structures. Specifically, their motility during quiescence and their reversibility upon exit from quiescence were tested. Most GFP-labeled foci formed during quiescence were irreversible, confirming previous work by other groups (Narayanaswamy *et al.*, 2009; O'Connell *et al.*, 2014). As expected, all proteasomal components accumulated in reversible cytosolic foci. GFP-labeled versions of proteins encoded by *ADE4*, *DNM1*, *DOA1*, *NEM1*, *PAK1*, *SET3*, *SNF1*, *SNF5*, *SNF6*, *SRO9*, *UBI4*, *UBP6*, and *VPS24*, whose deletions resulted in perturbed PSG formation, were also found to form cytosolic foci in quiescence (Table 1). To examine whether these cytosolic foci behave like PSGs, we tested their clearance upon exit from quiescence. With the exception of Ade4, Ubp6, and Ubi4, the cytosolic foci of all other gene products did not clear with the resumption of growth, showing that they did not behave like PSGs.

Only a small number of proteins, namely Ade16, Nam7, Kap95, Crm1, and Kap123, the latter three of which are members of the β-karyopherin family (Wozniak *et al.*, 1998), joined the list of proteins forming motile and reversible cytosolic foci in quiescence (Supplemental Table S2). None of them colocalized with PSGs (Supplemental Figure S4). Proteins known to be associated with the proteasomes, such as Ubp6 and Blm10, colocalized with PSGs (Figure 4, A and B). Colocalization studies of GFP-labeled Ubi4-GG, which was chromosomally deleted for the diglycine motif to avoid C-terminal cleavage of the GFP moiety from ubiquitin, and mCherry-labeled Pre2 suggested the presence of GFP-tagged ubiquitin within PSGs (Figure 4C). Western blot analysis confirmed the presence of GFP-tagged ubiquitin, which results from proteolytic processing of the polyubiquitin precursor Ubi4 during stationary phase (Figure 4C, panel labeled Ub-GG-GFP). Attempts to replenish (tagged versions of) ubiquitin in quiescent *ubp6*Δ and *ubi4*Δ cells by using *GAL1*, *ADH1*, *ADH2*, and *UBI4* promoter-driven plasmids failed, suggesting that the ubiquitin level is hardly manipulated in quiescence.

To investigate the structural organization of PSGs, we imaged cross-linked PSGs from wild-type cells expressing Rpn1-GFP via dSTORM (for enrichment of cross-linked PSGs, see Figure 5). The PSG signals appear as discrete isolated structures when imaged via wide-field total internal reflection fluorescence (TIRF) microscopy (Jain *et al.*, 2016) (Figure 4D, left panel). The nanoscale resolution achieved via dSTORM revealed a finer organization not readily observable by conventional microscopy (Figure 4D, right and bottom panels). Three-dimensional surface projections of a representative dSTORM image (Figure 4E) revealed a highly heterogeneous structure with a high number of overlapping single-molecule localizations at its center (dark blue). This area likely represents the core of the PSG with a diameter of ~200 nm, similar to that reported by immunoelectron microscopy (Laporte *et al.*, 2008), while single localizations at the periphery may arise from free proteasomes and/or

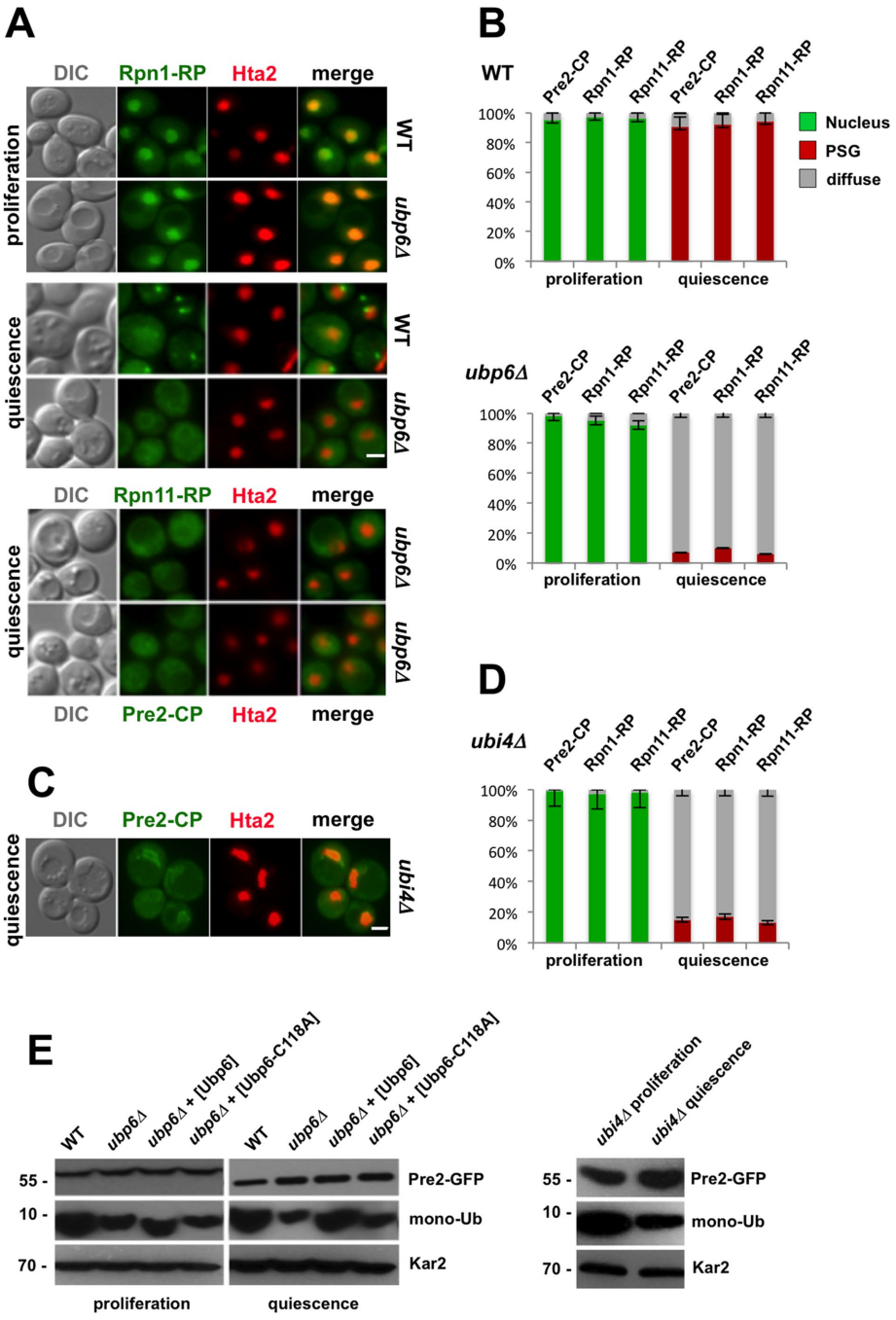

FIGURE 2: Proteasome localizations in *ubp6*Δ and *ubi4*Δ cells. (A) Direct fluorescence microscopy of wild-type and mutant *ubp6*Δ cells expressing RP base Rpn1-GFP and Hta2-mCherry during cell proliferation and quiescence (top panels). Direct fluorescence microscopy of quiescent *ubp6*Δ cells expressing either Pre2-GFP or PR lid Rpn11-GFP and Hta2-mCherry (bottom panel). Scale bar: 3 µm. (B) Fluorescence of Pre2-, Rpn1-, and Rpn11-GFP in proliferating and quiescent wild-type and *ubp6*Δ cells was scored as nuclear (green), diffuse (gray), or in PSGs (red); $n > 200$ cells, three experiments, error bars show SD. (C) Direct fluorescence microscopy of quiescent *ubi4*Δ cells expressing Pre2-GFP. Scale bar: 3 µm. (D) Fluorescence of Pre2-, Rpn1-, and Rpn11-GFP in quiescent *ubi4*Δ cells was scored as nuclear (green), diffuse (gray), or in PSGs (red); $n > 200$ cells, three experiments, error bars show SD. (E) Levels of free ubiquitin were detected in cell lysates by SDS–PAGE and Western blot using antibodies against ubiquitin and GFP. Kar2 was probed as loading control.

nonspecific antibody reactions. Around 700 localizations were detected per sample (20 samples) versus ~10,000 existing proteasomes in a yeast cell (Kulak *et al.*, 2014), suggesting a densely packed core in which the majority of GFP epitopes are sterically occluded and therefore not readily accessible for immunofluorescence. Alternatively, the finding of one-tenth of the proteasomes within the PSG sample could be explained by the fact that the PSGs were not isolated as intact organelles, collapsed during fixation, or do not contain all proteasomes of the cell.

Mass spectrometry–based approaches determine the protein composition of PSGs

To identify PSG-resident proteins in quiescent yeast cells, we used an integrated proteomic approach based on in vivo cross-linking of cells followed by lysis under denaturing conditions (Guerrero *et al.*, 2006; Kaake *et al.*, 2010). This cross-linking strategy was chosen because the PSG is a membrane-less droplet of soluble proteins (Laporte *et al.*, 2008). For retention of transiently interacting proteins within PSGs, quiescent cells were cross-linked by formaldehyde. The cross-linked cells were disintegrated in the presence of urea, and proteasomes were harvested by tandem-affinity purification using a dodeca-histidine tag combined with the in vivo biotinylation signal peptide sequence (HBH) on Pre2. Wild-type and *blm10*Δ cells with WCGa background were analyzed, because PSG formation occurs in nearly all wild-type cells and is abrogated in *blm10*Δ cells with regard to the CP (Weberruss *et al.*, 2013). Cross-linked quiescent cells from both strains were processed for tandem affinity purification. The eluates were analyzed by SDS–PAGE and Western blot before liquid chromatography–tandem mass spectroscopy (LC-MS/MS) analysis (Supplemental Figure S5). Possible PSG scaffold proteins should be identifiable through the comparison of the proteomic profiles of quiescent wild-type and *blm10*Δ cells. Two sets of duplicates were analyzed, and only peptides resolved in all four experiments were counted. As a control for nonspecific binding to the beads, lysates of cross-linked quiescent cells without HBH-tagged protein were subjected to tandem-affinity purification and LC-MS/MS analysis. In this control, no proteasomal peptides were isolated, but low numbers of peptides from metabolic enzymes and ribosomal subunits were identified (unpublished data), which usually arise from cross-linked and aggregation-prone proteins in quiescent cells (Narayanaswamy *et al.*, 2009; O'Connell *et al.*, 2014). The peptides of the control were subtracted from the peptides yielded from wild-type and *blm10*Δ cells expressing Pre2-HBH. High peptide counts resulted for the complete set of proteasomal subunits in

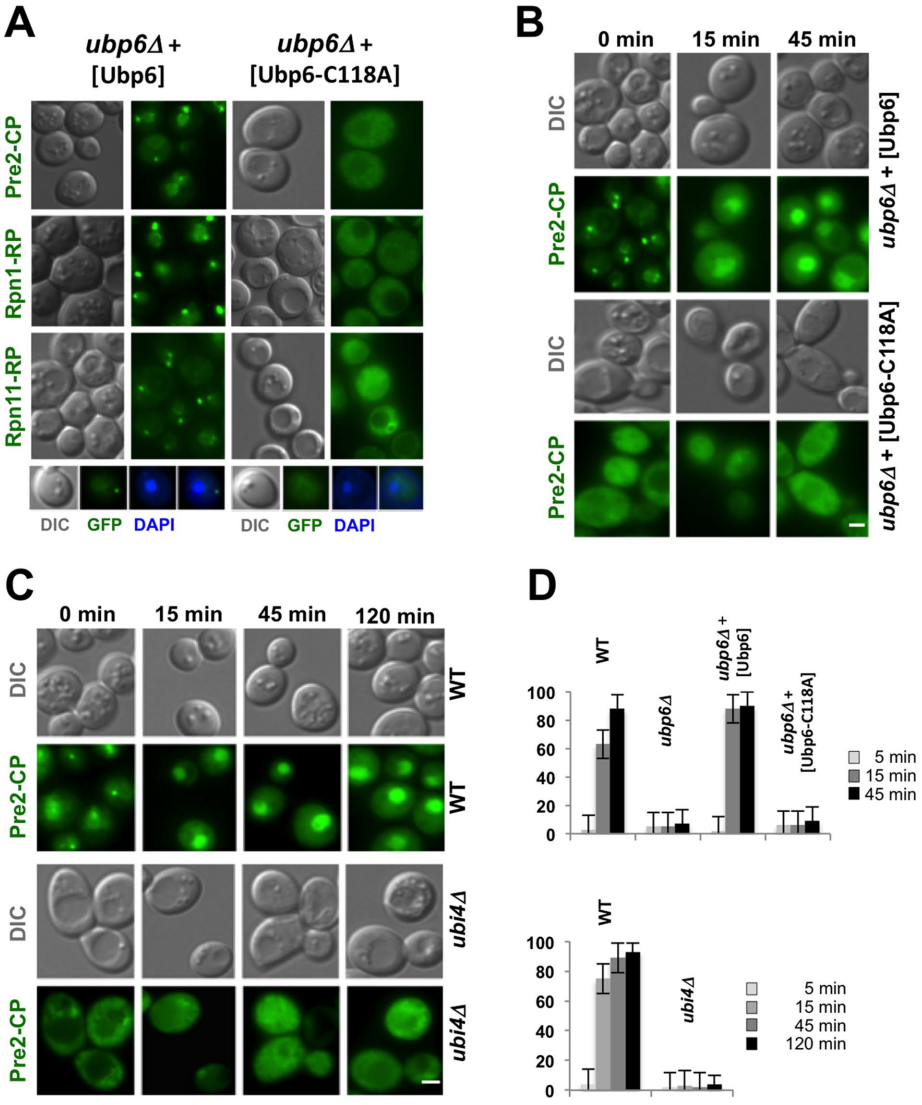

FIGURE 3: Nuclear recovery of GFP-labeled CP in *ubp6*Δ and *ubi4*Δ cells upon exit from quiescence. (A) Direct fluorescence microscopy of quiescent *ubp6*Δ cells expressing Pre2-, Rpn1-, and Rpn11-GFP, respectively, and complemented with plasmid-born expression of *UBP6* and *UBP6*-C118A (top, left panels). Representative cells are stained with DAPI to visualize the nuclei (bottom, left panels). Direct fluorescence microscopy (B) of *ubp6*Δ-*UBP6* and *ubp6*Δ-*UBP6*-C118A cells expressing Pre2-GFP and of (C) *ubi4*Δ cells expressing Pre2-GFP was performed at indicated time points upon exit from quiescence. Scale bar: 3 μm. (D) Numbers of cells with nuclear CP were scored at indicated time points; $n > 200$ cells, three experiments, error bars show SD.

wild type and *blm10*Δ. The proteomic profiles of wild-type and *blm10*Δ cells were identical, except that Blm10 was present in wild-type cells and absent from *blm10*Δ cells, and ubiquitin was enriched in wild type compared with *blm10*Δ (Supplemental Table S3). We also compared the proteomic proteasome profile of quiescent cells with previous profiles from proliferating cells using in vivo cross-linking of HBH-tagged proteasomal subunits (Guerrero *et al.*, 2006). No other protein except Blm10 was found to be present at high levels in quiescence compared with proliferation. The mass spectroscopy allowed the identification of ubiquitin but no ubiquitinylated peptides (L.H., unpublished observations).

Ubiquitin is a key component of proteasome storage granules

For analysis of the protein composition of PSGs in detail, cross-linked PSGs were enriched from quiescent BY4741 wild-type cells expressing GFPS (Strep-Tactin)-labeled Pre2 (Pre2-GFPS). Stepwise sucrose cushion ultracentrifugation yielded GFP-labeled PSGs, which cosedimented with fragments of 4′,6-diamidino-2-phenylindole (DAPI)-stained organelles as revealed by fluorescence microscopy (Figure 5A). Filter devices were used (as specified in the Supplemental Materials) to further separate the PSGs from DAPI-stainable nuclear and mitochondrial remnants (Figure 5B), as confirmed by Western blot analysis using antibodies against histone H3 and Tim23, a protein of the mitochondrial translocase complex. Also, markers of ribosomes (Rps6) and autophagosomes (Atg8) did not react with PSGs enriched by sucrose cushion ultracentrifugation followed by filtration (Figure 5C). The enriched PSGs were briefly boiled to reverse formaldehyde cross-links. SDS–PAGE followed by Coomassie blue staining of the released proteins revealed the typical banding pattern of CP subunits, which is identical to the banding pattern of purified CP (Figure 5D, top panel, compare lanes 1 and 2). High molecular mass subunits of the RP and Blm10 were detected by Western blot analysis after overnight heating at 65°C (Figure 5D, bottom panel, lane 3). Finally, bands in the range of 60–240 kDa were excised and analyzed by mass spectrometry. Pre2-GFP, Rpn1, and Blm10 were identified but did not migrate at the expected size due to the overnight treatment (unpublished data). Because PSGs do not form under conditions of ubiquitin depletion, we tested whether ubiquitin is present within PSGs. As a control, proteasome holo-enzymes were affinity purified as GFPS-labeled protein complexes from proliferating cells and probed for ubiquitin. Consistent with the literature (Besche *et al.*, 2014), polyubiquitin chains were detected on proteasome holo-enzymes trapped during protein degradation (Figure 5E, lanes 1 and 2).

Interestingly, polyubiquitinylated proteins were hardly detected within cross-linked PSGs that were heated in sample buffer overnight to release high molecular mass proteins (Figure 5E, lanes 3 and 4). Instead of polyubiquitin, free ubiquitin was enriched within PSGs. The presence of ubiquitin within purified PSGs was also verified by mass spectrometry by excising the ~8 kDa protein reacting with anti-ubiquitin antibodies (unpublished data).

Overexpression of lysine-less ubiquitin induces premature PSG formation and inhibits cell growth

For investigation of whether PSG formation is prematurely induced in proliferating cells by manipulating the level of free ubiquitin, the expression of His-tagged ubiquitin behind the *CUP1*-promoter was induced in wild-type cells expressing Pre2-GFP grown in YPD medium. As revealed by fluorescence microscopy, overnight overexpression of His-ubiquitin forced the sequestration of the CP into PSGs, while the CP remained nuclear in mock-treated cells with endogenous ubiquitin levels (Figure 6A, left panel). The expression of

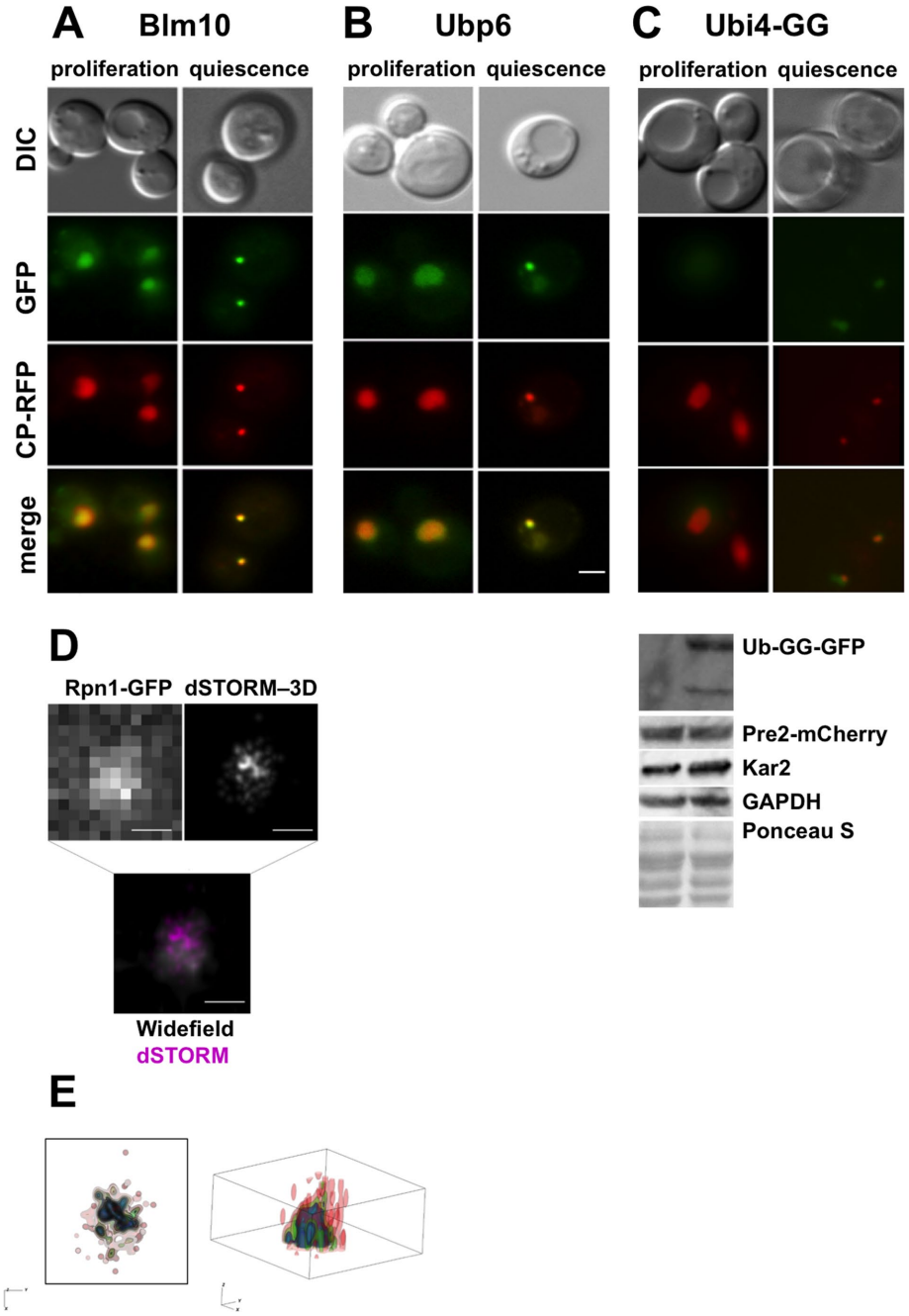

FIGURE 4: Fluorescence microscopy studies of PSGs. GFP-labeled versions of either (A) Blm10, (B) Ubp6, or (C) Ubi4 chromosomally harboring a C-terminal deletion of the C-terminal diglycine motif (–GG) and Pre2-mCherry were monitored in proliferating and quiescent yeast cells. Scale bar: 3 µm. Western blot analysis for ubiquitin-GG-GFP, the cleavage product of Ubi4-GG-GFP, Pre2-mCherry, Kar2, and GAPDH in proliferating and quiescent yeast. Ponceau S staining shows equal protein load (bottom panel). (D) Wide-field HiLo fluorescence image of a single PSG core obtained from a cross-linked PSGs, enriched from wild-type cells expressing Rpn1-GFP (left). Three-dimensional projection of the corresponding dSTORM image generated with Alexa Fluor 647–anti-GFP (right). Overlay of the wide-field HiLo and dSTORM images (bottom). The wide-field HiLo image was rescaled and smoothed to a pixel size of 10 nm for compatibility with the dSTORM image. (E) Surface projection renderings of the dSTORM reconstruction. Areas of dark blue indicate a relative high density of single-molecule localizations. Scale bars: 500 nm.

His-ubiquitin was confirmed by Western blot (Figure 6A, right panel). Additionally, we tested the effect of lysine-less (K0) ubiquitin in which all lysines are mutated to arginines and the C-terminal diglycine motif is deleted (–GG), so that it is not linkable to any substrate or proceeding ubiquitin molecule. Among pleiotropic effects, K0 ubiquitin inhibits proteasomal degradation (Bloom *et al.*, 2003; Ziv *et al.*, 2011). Again, K0 ubiquitin-GG was overexpressed behind the *CUP1* promoter in wild-type cells expressing Pre2-GFP. After a few hours in YPD, PSGs were formed, and cell cycle progression was arrested, whereas mock-treated cells proliferated with continuous nuclear localization of proteasomes (Figure 6B). The cells forming PSGs upon K0 ubiquitin overexpression were serially diluted and spotted on YPD medium with and without copper. The cells did not resume growth on copper-containing medium, suggesting that K0 ubiquitin interferes with cell cycle progression. As a control, cells containing wild-type ubiquitin grew on copper-containing medium (Figure 6C).

Ideally, the overexpression of ubiquitin variants would have been performed in quiescent *ubi4*Δ cells. However, protein overexpression is only feasible in proliferating cells, where proteasomes are located in the nucleus independent of the genetic background. Galactose-induced overexpression of Ubi4 in *ubi4*Δ cells yielded unprocessed Ubi4, suggesting that the ubiquitin-processing hydrolase is not active during proliferation (unpublished data).

Proteasome holo-enzymes are unstable in quiescence

As is well known from the literature, proteasome holo-enzymes remain stable in the presence of ATP and during the degradation of polyubiquitinylated substrates (Kleijnen *et al.*, 2007; Kriegenburg *et al.*, 2008). With the decline of ATP, proteasome holo-enzymes tend to dissociate. Thus proteasome holo-enzymes are unstable in quiescent cells (Bajorek *et al.*, 2003). For testing this in our set of mutants, lysates of wild-type and mutant cells were subjected to native PAGE and analyzed by fluoroimaging of the GFP moieties attached to either CP, RP base, or RP lid subunit. Proteasome configurations were assigned according to our previous analysis using specific antibodies and mass spectrometry (Supplemental Figure S6) (Enenkel, 2012). Because *ubp6*Δ cells displayed one of the most striking phenotypes with regard to orchestrating PSG organization, we depicted proteasome configurations from proliferating and quiescent *ubp6*Δ cells. Proteasome holo-enzymes with either RP–CP–RP or RP–CP configuration were present in proliferating cells (Figure 7A) and dissociated into RP and CP in quiescent cells (Figure 7B). In wild type, a considerable fraction of CP was bound to Blm10. In quiescent *ubp6*Δ cells, the overall proteasome configurations were similar to wild type, but less Blm10 was bound to the CP (Figure 7,

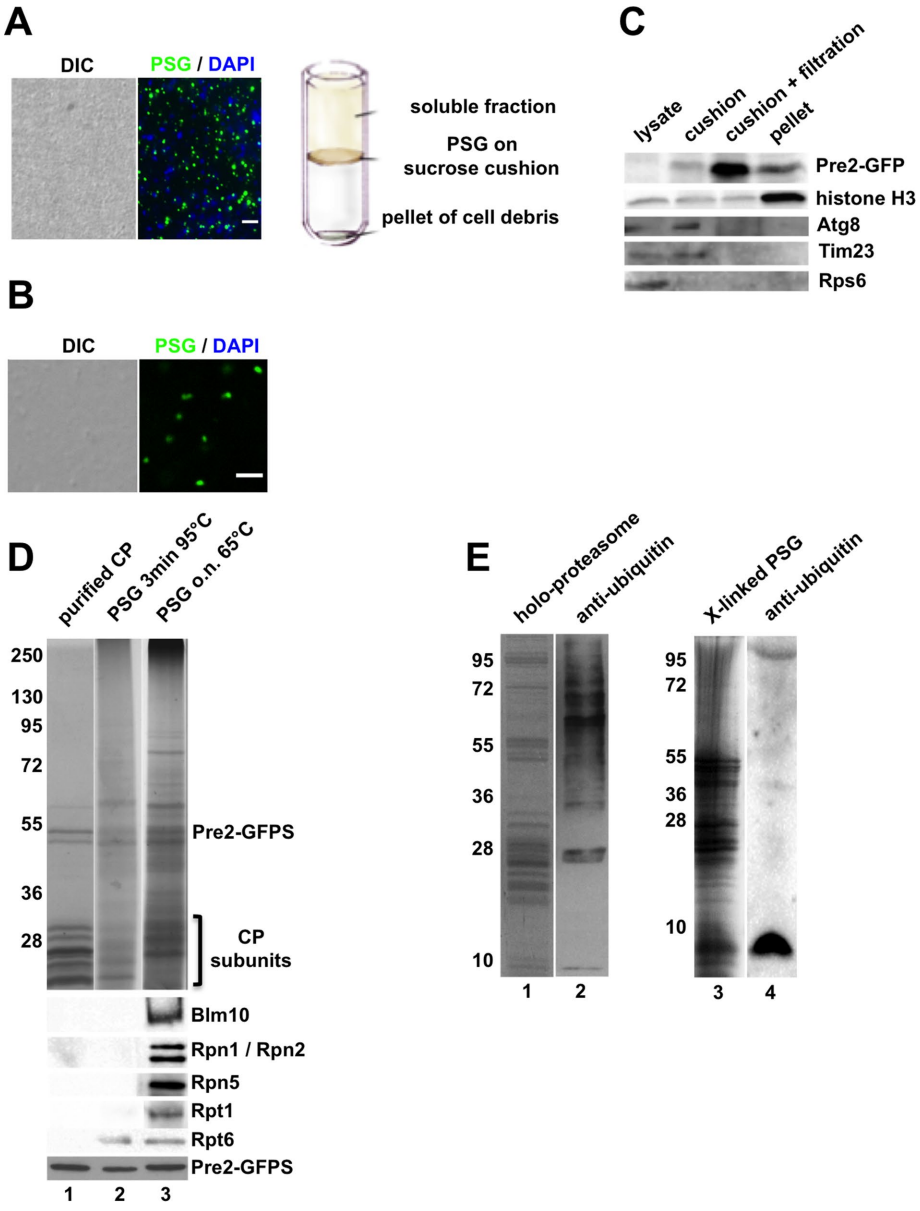

FIGURE 5: Determination of protein composition of PSGs. (A) Sucrose cushion ultracentrifugation for PSG enrichment. Lysates of cross-linked wild-type cells expressing Pre2-GFPS were subjected to sucrose cushion ultracentrifugation. PSGs were harvested from the layer on top of the 2 M sucrose cushion and analyzed by fluorescence microscopy. GFP-labeled PSGs do not coincide with nuclear structures stained by DAPI. DIC was used to monitor the sample homogenization. Scale bar: 1 µm. (B) Filtered PSG samples containing GFP-labeled CP were stained with DAPI and monitored by fluorescence microscopy. Scale bar: 1 µm. (C). Cell equivalents of crude lysate and ultracentrifugation fractions before and after filtration were subjected to SDS–PAGE and Western blotting using specific antibodies against Pre2-GFP, histone H3, Atg8, Tim23, and Rps6. Note that formaldehyde cross-links are reversed by boiling in sample buffer. (D) The protein banding pattern of purified GFP-labeled CP (lane 1) was compared with filtered PSGs by SDS–PAGE, Coomassie blue staining (top panel), and Western blotting (bottom panel). Cross-linked PSGs were either boiled for 3 min at 95°C (lane 2) or heated overnight at 65°C to release high molecular mass proteins (lane 3). Blm10, Rpn1, Rpn2, Rpn5, Rtp1, Rpt6, and Pre2-GFP were detected by specific antibodies (bottom panel). (E) Proteasome holo-enzymes were affinity purified by Pre2-GFPS in the presence of 100 µm MG132 and subjected to SDS–PAGE. Coomassie blue staining revealed the protein banding pattern of the RP and CP subunits (lane 1). Polyubiquitin chains (high molecular mass range) and traces of free ubiquitin (8 kDa) were detected by Western blot (lane 2). Filtered PSGs were heated overnight in sample buffer and subjected to SDS–PAGE and either stained with Coomassie blue (lane 3) or blotted against ubiquitin (lane 4).

bottom panel). Because the sequestration of the CP into PSGs is facilitated by Blm10 (Weberruss *et al.*, 2013), diminished fractions of Blm10–bound CP may contribute to perturbed PSG organization in addition to low ubiquitin levels in *ubp6*Δ mutants. Consistent with our finding in *ubp6*Δ cells, our hit mutants with disturbed PSG formation showed RP and CP dissociated as well, confirming that the decline of ATP has a critical influence on proteasome stability during quiescence (selection of hit mutants, Supplemental Figures S7 and S8).

DISCUSSION

Here we explored different approaches to understand PSG organization and to identify key proteins apart from proteasomal components that are required to assemble these reversible and motile granules in the cytoplasm of quiescent yeast cells.

Our initial high-throughput screen for yeast null mutants with perturbed PSGs identified Blm10, a protein required for CP but not RP sequestration into PSGs (Weberruss *et al.*, 2013) (Supplemental Table S1). To identify proteins that orchestrate the sequestration of both the CP and RP into PSGs, we extended our array to mutants with defective RP sequestration into PSGs (Table 1). The proteins affected in these mutants have diverse functions, being either involved in phosphorylation, the regulation of metabolic energy, genotoxic stress response, or ubiquitin regulation. Npr3 kinase, which acts on TORC1 kinase, Pak1, the upstream kinase of AMP-dependent kinase Snf1, and Snf1 kinase emerged in our extended screen for mutants with reduced PSG formation. TORC1 and Pak1 govern the sensing of glucose depletion in quiescence (Zhang *et al.*, 2011) and may modify proteasomal components by phosphorylation, thus influencing proteasome dynamics and their propensity to assemble into PSGs. Eighteen kinases have been reported to form reversible cytosolic foci in quiescence, although Npr3, Pak1, and Snf1 were not among them (Shah *et al.*, 2014). None of these kinases including Npr3, Pak1, and Snf1, colocalized with PSGs, and none of them were identified in our mass spectrometry analysis of cross-linked PSGs. However, it is interesting to note that the phenotypes of quiescent yeast cells lacking either kinase granules or PSGs are similar. Both displayed reduced fitness in chronological aging, suggesting that the global reorganization of various enzymes into cytosolic foci is beneficial for the longevity and reversibility of quiescence (Shah *et al.*, 2014).

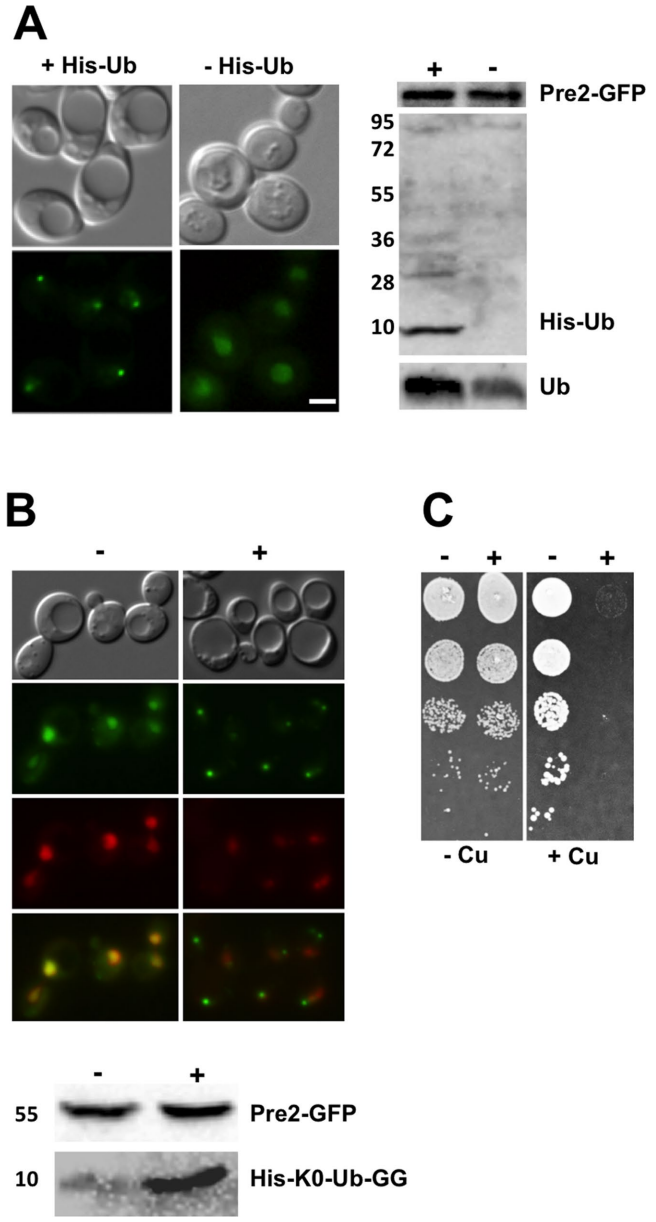

FIGURE 6: Overexpression of ubiquitin induces premature PSG formation. (A) Wild-type cells containing a plasmid for *CUP1*-promoter driven expression of His-tagged ubiquitin (His-Ub) were grown to early logarithmic phase (OD ~ 0.3) in YPD medium and induced overnight with copper (+) or mock treated (–). Cells were monitored by direct fluorescence microscopy (left panel). Scale bar: 3 µm. Lysates were subjected to SDS–PAGE and probed for Pre2-GFP, endogenous Ub or episomally expressed His-Ub (right panel). (B) Wild-type cells harboring a plasmid for *CUP1*-promoter driven expression of His-tagged K0 Ub-GG were grown to early logarithmic phase in YPD and either induced with copper for few hours or mock treated. Cells were monitored by direct fluorescence microscopy. Scale bar: 3 µm. Total cell lysates were subjected to SDS–PAGE, blotted, and probed with anti-GFP and anti-His antibodies. (C) Serial dilutions of wild-type cells harboring the expression plasmid for *CUP1*-driven K0 Ub expression were spotted on YPD medium either containing or lacking 200 µM copper.

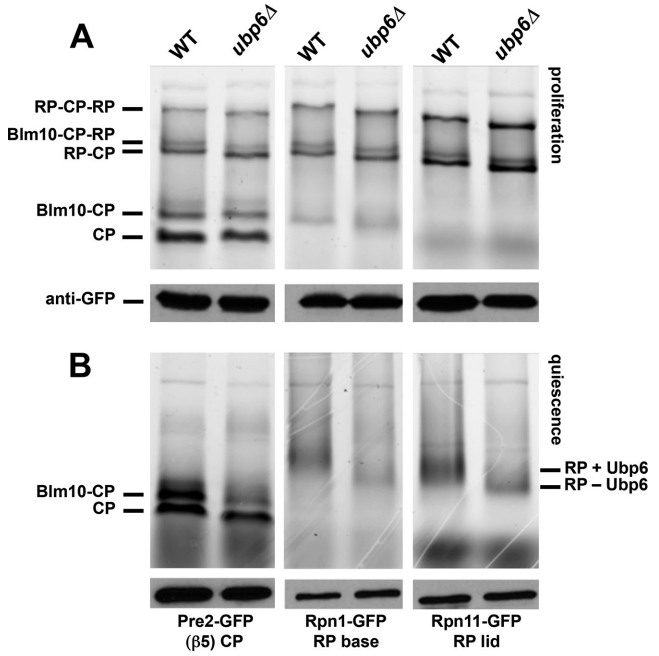

FIGURE 7: Proteasome complexes in proliferating and quiescent wild-type and *ubp6*Δ cells. (A) Lysates of proliferating wild-type and *ubp6*Δ cells expressing either Pre2-, Rpn1-, or Rpn11-GFP were subjected to native PAGE. The GFP moieties of the CP and RP were visualized by fluoroimaging. Proteasome configurations were assigned to RP-CP-RP, Blm10-CP-RP, RP-CP, Blm10-CP, and CP as previously elaborated (Enenkel, 2012). The protein loaded to each lane was analyzed by SDS–PAGE followed by Western blotting using anti-GFP antibodies. (B) Lysates of quiescent wild-type and *ubp6*Δ cells expressing the proteasomal reporter proteins above were subjected to native PAGE. Again, CP and RP species were visualized by GFP imaging and assigned to RP, Blm10-CP, and CP, as previously elaborated (Weberruss *et al.*, 2013). The protein load to each lane was detected, as above. Note that, in *upb6*Δ cells, the RP migrates slightly faster than in wild type due to the lack of Ubp6.

The CCAAT transcription factor complex is a global regulator of respiratory gene expression that is repressed by glucose. Our high-throughput imaging screen identified Hap subunits of the CCAAT transcription factor, which mirrors metabolic changes during the diauxic shift from glycolysis to gluconeogenesis (Zampar *et al.*, 2013). Dnm1, a short-lived GTPase regulating mitochondrial fission during diauxic shift, was identified as well. The half-life of Dnm1 depends on Blm10 (Tar *et al.*, 2014), linking two hit proteins of our high-throughput analysis.

All hit genes listed in the complete set of data (see the Supplemental Material) showed biological variability with regard to their impact on PSG formation. Thus we focused our efforts on those genes, in which the sequestration of CP and RP into PSGs was almost abrogated. These genes, namely *UBP6* and *UBI4*, encode proteins regulating ubiquitin concentration. Disturbed PSG formation as displayed by *ubp6*Δ and *ubi4*Δ mutants correlated with significantly decreased levels of free ubiquitin, which below a yet unknown threshold abrogates PSG formation. Ubp6, an ubiquitin-specific hydrolase associated with the RP base, aids to replenish the pool of free ubiquitin and modifies protein substrates by trimming branched polyubiquitin chains (Crosas *et al.*, 2006; Hanna *et al.*, 2006), specifically by catalyzing the removal of supernumerary polyubiquitin chains (Lee *et al.*, 2016). Its activity contributes to PSG formation, supporting our assumption that proteasomes devoid of branched polyubiquitin chains are preferentially sequestered into PSGs. Mutations in Rpn11, the RP lid subunit responsible for the removal of ubiquitin moieties from polyubiquitinylated substrates, lead to nuclear retention of proteasomes and impaired PSG formation (Saunier

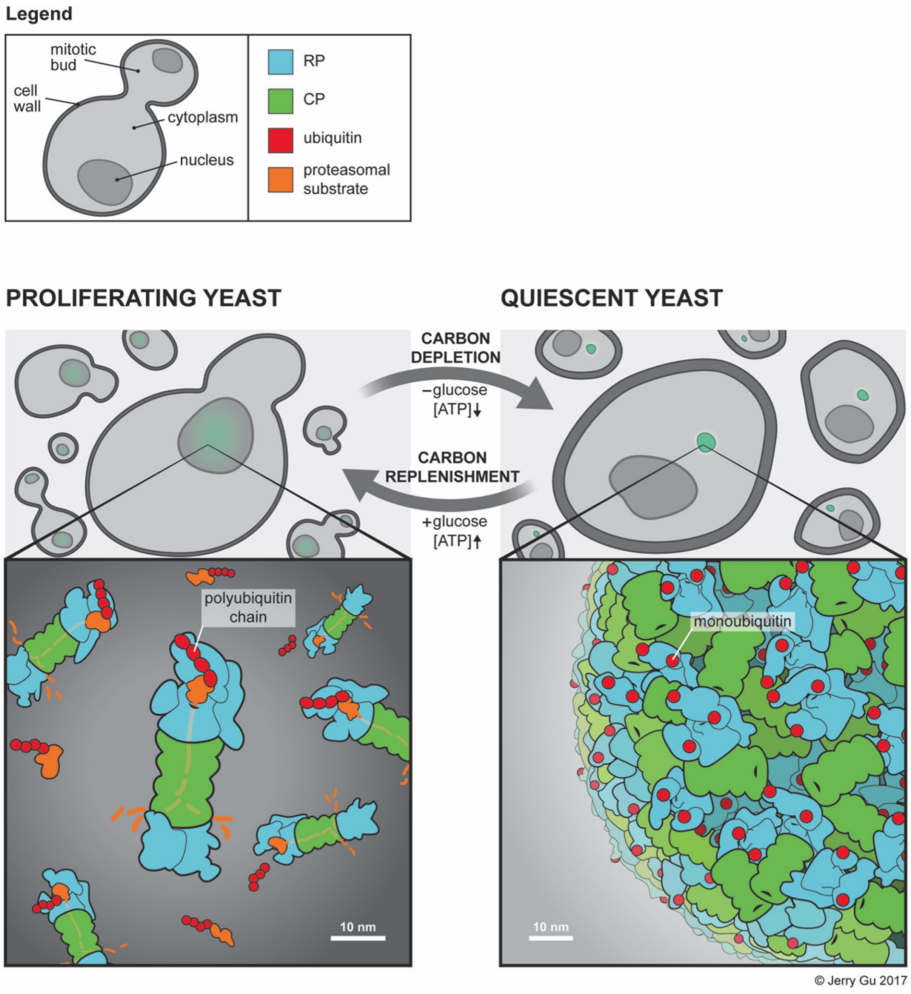

FIGURE 8: Model of PSG organization and proteasome dynamics between proliferation and quiescence. In proliferating cells in which the ATP level is high, proteasome holo-enzymes mainly occur in the nucleus and are engaged in the degradation of polyubiquitinylated proteins. During transition to quiescence, glucose is depleted, the ATP level declines, and fewer proteins might be degraded in the nucleus. Proteasomes migrate to the nuclear envelope and exit the nucleus, most likely through nuclear pores. PSGs are formed and move as membrane-less entities through the cytoplasm. Because proteasome holo-enzymes are less stable at low ATP concentration, RP and CP might be separately stored within PSGs. RP, CP, and mono-ubiquitin are major constituents of the PSGs. With the addition of glucose, cells receive the signal to resume growth. The ATP level increases, and PSGs dissolve within a few minutes. Proteasomes are rapidly relocated to the nucleus, where ubiquitin-dependent proteolysis of short-lived proteins promotes cell cycle progression.

et al., 2013). Furthermore, the lack of Hul5, which works as an antagonist of Ubp6 by elongating polyubiquitin chains (Finley, 2011), leads to proteasomes loaded with polyubiquitin chains, their retention in the nucleus, and consequently, reduced PSG formation (van Deventer *et al.*, 2015).

On the basis of these findings we propose the following model in which proteasomes loaded with polyubiquitin chains are mainly localized in the nucleus, where a major need for proteasomal protein degradation seems to be required during cell proliferation. The release of polyubiquitin chains and the presence of mono-ubiquitin trigger nuclear export and the sequestration of proteasomes into PSGs (Figure 8). The decline of ATP in quiescence impacts the stability of proteasome holo-enzymes, suggesting that proteasomes do not exist as holo-enzymes within PSGs. They are rather dissociated into RP and CP with a significant fraction bound to Blm10, which facilitates CP sequestration into the PSG and its reimport into the nucleus upon exit from quiescence. Mono-ubiquitin is a crucial component for the formation of PSGs. Its overexpression, especially if ubiquitin cannot be conjugated to a growing polyubiquitin chain, induces premature PSG formation in proliferating cells.

Interestingly, proteasome inhibition and conditional mutations within the proteasome cause cell cycle arrest and the formation of reversible proteasome granules, named JUNQ (Kaganovich *et al.*, 2008), close to the nuclear envelope. These observations support our model that proteasomes with polyubiquitin chains and inhibited during degradation remain stuck at the nuclear envelope.

None of our hit proteins, except proteins of the ubiquitin–proteasome system, colocalized with the PSGs. This is consistent with other work showing that most cytosolic foci induced by thermal, chemical, and nutritional stress are not composed of multisubunit complexes. From a selection of ~800 cytosolic proteins, nearly 200 proteins reside in irreversible foci and do not colocalize with enzymes participating in the same metabolic pathway. Mass spectrometry analysis of these foci did not yield peptides from proteasomal subunits (O'Connell *et al.*, 2014), but rather peptides overlapping with those detected in our untagged cells used as control (Guerrero *et al.*, 2006). Stress granules, as analyzed in an approach similar to ours (Wallace *et al.*, 2015; Jain *et al.*, 2016), did not contain proteasomal components, further supporting the conclusion that PSGs are unique reservoirs of ubiquitin and proteasomes, which according to our dSTORM analysis are densely packed into granules. This reservoir of key components of the ubiquitin–proteasome system can be instantaneously mobilized with the resumption of growth. PSGs dissolve, and mature proteasomes are translocated within minutes into the nucleus to degrade polyubiquitinylated proteins. The synthesis of new proteins and degradation of short-lived proteins (e.g., cell cycle regulators) resume with the exit from quiescence. In contrast to proliferating cells with high ATP levels, quiescent cells experience an austerity budget, and protein homeostasis is adjusted to the economic challenge of decreased ATP levels. Therefore we assume that quiescence lasts with less degradation of polyubiquitinylated proteins. Protein synthesis is stalled, and fewer short-lived proteins accrue as polyubiquitinylated substrates.

It still remains a mystery how proteasomes and ubiquitin separate in PSGs in the aqueous environment of the cytoplasm. Recent studies show that the cytoplasmic fluidity changes between the metabolically active and dormant state of cells. Accordingly, the motion of intracellular components may become disproportionally constrained with increasing size during the transition from proliferation to quiescence

(Parry *et al.*, 2014; Munder *et al.*, 2016). However, PSG organization may be driven not only by extrinsic changes in the solvent structure but also by intrinsic features of the solute protein. Proteins that tend to undergo liquid–liquid phase separations in an aqueous environment are often intrinsically disordered (Marsh and Forman-Kay, 2010; Brangwynne, 2013). How proteasomes follow this concept of liquid–liquid phase separation is to be tested, because their subunits are folded proteins with only a few intrinsically disordered domains (Aufderheide *et al.*, 2015). Intrinsically disordered proteins are even at risk of being degraded by the proteasomes (Liu *et al.*, 2003) if they serve as PSG scaffolds. Future reconstitution assays of PSGs using CP and RP components and ubiquitin followed by biophysical investigations of protein conformations will shed light into molecular dynamics of proteasomes, which seem to exist either as freely diffusible protein complexes or as condensed particles in a liquid droplet.

MATERIALS AND METHODS

Automated image acquisition

PCR-based homologous recombination (Tong *et al.*, 2001) was used to create the query strain expressing Pre2-GFP, *RPL39*pr-tdTomato, and Hta2-mCherry. The query strain was mated to the collection of yeast deletion strains by replica pinning (Giaever *et al.*, 2002). Diploids were selected and sporulated using standard selection strategies (Tong *et al.*, 2001). The *gene*xΔ haploids expressing Pre2-GFP, *RPL39*pr-tdTomato, and Hta2-mCherry were isolated through successive pinning onto selective media lacking histidine, uracil, leucine, arginine, and lysine, but supplemented with canavanine, *S*-(2-aminoethyl)-L-cysteine hydrochloride, geneticin, and nourseothricin. Then cells were transferred into liquid YPD by using the RAININ Liquidator96 manual benchtop pipetting system (Mettler Toledo). Antibiotics were omitted, as they impact the growth to stationary phase. Cells were grown overnight in 96-well plates covered with Breathe Easy Sealing Tape (E&K Scientific) before they were diluted by 1:3 in 500 µl YPD in 96–deep well plates and incubated for 5 d in at a 30° angle, 220 rpm, and 30°C. For optimization of cell density and elimination of autofluorescence of aged YPD for image analysis, each subculture was diluted in sterile water at 1:100 and transferred into Greiner 96-well plates. The optical density at 600 nm (OD_{600}) was measured using the spectrophotometer Synergy2 (BioTek). Gen5 software was used to calculate the average cell density, and adjusted volumes were transferred to a 384-well CellCarrier glass slide (PerkinElmer; 6007558) for high-throughput imaging with the Evotec Opera microscope, an automated spinning-disk confocal microscope equipped with a 60×/1.2 NA water-immersion objective (Perkin Elmer-Cetus). GFP was detected at 488-nm laser excitation and with 520/535-nm emission filters. mCherry and tdTomato (red fluorescent protein [RFP]) were detected at 561-nm laser excitation and with 600/40-nm emission filters. An exposure time of 800 ms and laser-based autofocusing were used. For each mutant strain, four fields in a well were imaged. Images were stored as proprietary multipage 16-bit TIFF files called FLEX files.

For image analysis, cells and nuclei were defined using CellProfiler software. The open-source image-analysis software CellProfiler (version 2.0.10415) was downloaded from www.cellprofiler.org. On each imaging plate, the query wild-type strain was spotted as a reference for PSG formation.

In addition to the automated image analysis, three individuals manually re-examined the micrographs. Four micrographs of each strain with at least 200 cells in total were evaluated. The mutant was counted as a hit when all three individuals independently found matching results in agreement with the results from the automated image analysis.

Yeast strains used in this study

All the strains used in the high-throughput array are isogenic to BY4741. The relevant genotypes are listed in Supplemental Table S4. GFP, tdTomato, and mCherry fusions were constructed using one-step PCR-mediated homologous recombination (Longtine *et al.*, 1998). All genes listed in Supplemental Table S1 were confirmed to be chromosomally deleted in the respective mutant by using PCR. The expression of fluorescent protein-labeled proteins was confirmed by Western blot analysis. Antibodies against Rpn1 and Rpn2 were kindly provided by Michael Glickman (Technion, Haifa, Israel), against Rpt1 and Rpt6 by Carl Mann (University of Paris-South, France), and against Tim23 by Angus McQuibban (University of Toronto, Canada). The source of anti-Blm10, Kar2 and Rpn5 antibodies is described previously (Weberruss *et al.*, 2013). Monoclonal mouse antibodies against GFP and mCherry were purchased from Clontech, against RGS-His from Qiagen, polyclonal rabbit antibodies against RPS6, Histone H3, and anti-GAPDH-HRP conjugates were from Abcam and antibodies against ubiquitin (BML-UG9511) from Enzo. Before blocking and adding antibodies blots were always stained with either Amido Black or Ponceau S to test for equal protein load.

Fluorescence microscopy

Manual fluorescence microscopy was performed with an AxioVision fluorescence microscope (Zeiss) equipped with the 100/1.4 oil-immersion objective lens (Plan-Apochromat) and the HBO103W/2 mercury vapor short-arc lamp. The GFP fluorescence was observed with an excitation maximum of 488 nm and an emission maximum of 520 nm, and the RFP fluorescence with an excitation maximum of 595 nm and an emission maximum of 615 nm. Images were taken with the Hamamatsu Orca-ER digital camera using Velocity software (Improvision). tdTomato cannot be visualized by using these settings and can only be viewed with the Evotech high-throughput microscope.

The resumption of growth after quiescence was induced by adding fresh YPD, and the protein dynamics were immediately monitored by fluorescence microscopy within a time frame of 10–30 min, as described previously (Weberruss *et al.*, 2013).

dSTORM sample preparation, imaging, and analysis

Cross-linked PSGs were isolated from wild-type cells expressing Rpn1-GFP and stained with an anti-GFP single-domain antibody (ChromoTek gt-250) conjugated with Alexa Fluor 647. Single-molecule localization microscopy was performed on a home-built superresolution epifluorescence/TIRF microscope comprising an Olympus IX-83 inverted fluorescence microscope base equipped with a 100×/1.49 NA oil-immersion UPAON objective lens; a 100-mW, 643-nm DPSS laser (Ultralasers); and a Cy5 filter set (Chroma). Imaging was performed with laser configuration in a highly inclined and laminated optical sheet (HiLo). A cylindrical lens (LK1002L1-A f = –1000, Thorlabs) was placed in the emission path between the microscope body and the camera to induce asymmetry in the *x* and *y* focal planes, allowing for estimation of the *z*-position of single-molecule localizations via the astigmatism method (Huang *et al.*, 2008). Five thousand frames were captured for each sample at a sampling rate of 50 Hz. Images were acquired in MicroManager (v.1.4.23) using a Photometrics QuantEM EMCCD (multiplier gain = 100). Raw data were processed and superresolution reconstructions were generated with the ImageJ plug-in ThunderSTORM using a maximum-likelihood estimation and multi-emitter fitting for subpixel localizations. Three-dimensional surface renderings were generated with VisIt (Lawrence Livermore National Laboratory).

Proteomic analysis of PSGs in quiescent yeast cells

The affinity purification of HBH- and GFPS-labeled CP and the enrichment of PSGs from formaldehyde cross-linked cells are described in detail in the Supplemental Material. The proteomic analysis was performed according to previous protocols (Guerrero *et al*., 2006; Kaake *et al*., 2010).

CUP1-induced overexpression of His-tagged versions of ubiquitin was performed as described previously (Finley *et al*., 1994). Cells transformed with an episomal plasmid were grown on selective synthetic complete medium. Copper induction of protein expression was done in YPD.

ACKNOWLEDGMENTS

We thank Brenda Andrews for her generous support in providing us with the collection of yeast strains and allowing us to access high-throughput technologies used in systems biology. We thank Sarina Norell, Alexandra Höfler, Amatullah Fatehi, and Esraa Elnagdi for their contributions to experiments. We thank Marion Schmidt, Youming Xie, and Dan Finley for providing plasmids and strains. Special thanks go to Julianne Burcoglu and Dieter H. Wolf (University of Stuttgart) for critical discussions and support. This work was supported by grants from the Deutsche Forschungsgemeinschaft/German Research Foundation (EN301-7/1), National Sciences and Engineering Research Council of Canada (4422666-2011), and Canadian Institutes for Health Research (325477) to C.E. and from the National Institutes of Health (R01GM074830) to L.H.

REFERENCES

Amen T, Kaganovich D (2015). Dynamic droplets: the role of cytoplasmic inclusions in stress, function, and disease. Cell Mol Life Sci 72, 401–415.

Aufderheide A, Unverdorben P, Baumeister W, Forster F (2015). Structural disorder and its role in proteasomal degradation. FEBS Lett 589, 2552–2560.

Bajorek M, Finley D, Glickman MH (2003). Proteasome disassembly and downregulation is correlated with viability during stationary phase. Curr Biol 13, 1140–1144.

Baumeister W, Walz J, Zuhl F, Seemuller E (1998). The proteasome: paradigm of a self-compartmentalizing protease. Cell 92, 367–380.

Besche HC, Sha Z, Kukushkin NV, Peth A, Hock EM, Kim W, Gygi S, Gutierrez JA, Liao H, Dick L, Goldberg AL (2014). Autoubiquitination of the 26S proteasome on Rpn13 regulates breakdown of ubiquitin conjugates. EMBO J 33, 1159–1176.

Bloom J, Amador V, Bartolini F, DeMartino G, Pagano M (2003). Proteasome-mediated degradation of p21 via N-terminal ubiquitinylation. Cell 115, 71–82.

Boone C, Bussey H, Andrews BJ (2007). Exploring genetic interactions and networks with yeast. Nat Rev Genet 8, 437–449.

Brangwynne CP (2013). Phase transitions and size scaling of membrane-less organelles. J Cell Biol 203, 875–881.

Chernova TA, Allen KD, Wesoloski LM, Shanks JR, Chernoff YO, Wilkinson KD (2003). Pleiotropic effects of Ubp6 loss on drug sensitivities and yeast prion are due to depletion of the free ubiquitin pool. J Biol Chem 278, 52102–52115.

Ciechanover A, Brundin P (2003). The ubiquitin proteasome system in neurodegenerative diseases: sometimes the chicken, sometimes the egg. Neuron 40, 427–446.

Cohen-Kaplan V, Livneh I, Avni N, Fabre B, Ziv T, Kwon YT, Ciechanover A (2016). p62- and ubiquitin-dependent stress-induced autophagy of the mammalian 26S proteasome. Proc Natl Acad Sci USA 113, E7490–E7499.

Crosas B, Hanna J, Kirkpatrick DS, Zhang DP, Tone Y, Hathaway NA, Buecker C, Leggett DS, Schmidt M, King RW, *et al.* (2006). Ubiquitin chains are remodeled at the proteasome by opposing ubiquitin and deubiquitinating activities. Cell 127, 1401–1413.

De Virgilio C (2012). The essence of yeast quiescence. FEMS Microbiol Rev 36, 306–339.

Doherty KM, Pride LD, Lukose J, Snydsman BE, Charles R, Pramanik A, Muller EG, Botstein D, Moore CW (2012). Loss of a 20S proteasome activator in *Saccharomyces cerevisiae* downregulates genes important for genomic integrity, increases DNA damage, and selectively sensitizes cells to agents with diverse mechanisms of action. G3 (Bethesda) 2, 943–959.

Enenkel C (2012). Using native gel electrophoresis and phosphofluoroimaging to analyze GFP-tagged proteasomes. Methods Mol Biol 832, 339–348.

Enenkel C (2014). Proteasome dynamics. Biochim Biophys Acta 1843, 39–46.

Finley D (2011). Misfolded proteins driven to destruction by Hul5. Nat Cell Biol 13, 1290–1292.

Finley D, Ozkaynak E, Varshavsky A (1987). The yeast polyubiquitin gene is essential for resistance to high temperatures, starvation, and other stresses. Cell 48, 1035–1046.

Finley D, Sadis S, Monia BP, Boucher P, Ecker DJ, Crooke ST, Chau V (1994). Inhibition of proteolysis and cell cycle progression in a multiubiquitination-deficient yeast mutant. Mol Cell Biol 14, 5501–5509.

Giaever G, Chu AM, Ni L, Connelly C, Riles L, Véronneau S, Dow S, Lucau-Danila A, Anderson K, André B, *et al.* (2002). Functional profiling of the *Saccharomyces cerevisiae* genome. Nature 418, 387–391.

Goldberg AL (2003). Protein degradation and protection against misfolded or damaged proteins. Nature 426, 895–899.

Gray JV, Petsko GA, Johnston GC, Ringe D, Singer RA, Werner-Washburne M (2004). "Sleeping beauty": quiescence in *Saccharomyces cerevisiae*. Microbiol Mol Biol Rev 68, 187–206.

Guerrero C, Tagwerker C, Kaiser P, Huang L (2006). An integrated mass spectrometry-based proteomic approach: quantitative analysis of tandem affinity-purified in vivo cross-linked protein complexes (QTAX) to decipher the 26 S proteasome-interacting network. Mol Cell Proteomics 5, 366–378.

Haller S, Garibotto V, Kovari E, Bouras C, Xekardaki A, Rodriguez C, Lazarczyk MJ, Giannakopoulos P, Lovblad KO (2013). Neuroimaging of dementia in 2013: what radiologists need to know. Eur Radiol 23, 3393–3404.

Hanna J, Hathaway NA, Tone Y, Crosas B, Elsasser S, Kirkpatrick DS, Leggett DS, Gygi SP, King RW, Finley D (2006). Deubiquitinating enzyme Ubp6 functions noncatalytically to delay proteasomal degradation. Cell 127, 99–111.

Hanna J, Meides A, Zhang DP, Finley D (2007). A ubiquitin stress response induces altered proteasome composition. Cell 129, 747–759.

Huang B, Wang W, Bates M, Zhuang X (2008). Three-dimensional super-resolution imaging by stochastic optical reconstruction microscopy. Science 319, 810–813.

Huh WK, Falvo JV, Gerke LC, Carroll AS, Howson RW, Weissman JS, O'Shea EK (2003). Global analysis of protein localization in budding yeast. Nature 425, 686–691.

Jain S, Wheeler JR, Walters RW, Agrawal A, Barsic A, Parker R (2016). ATPase-modulated stress granules contain a diverse proteome and substructure. Cell 164, 487–498.

Kaake RM, Milenkovic T, Przulj N, Kaiser P, Huang L (2010). Characterization of cell cycle specific protein interaction networks of the yeast 26S proteasome complex by the QTAX strategy. J Proteome Res 9, 2016–2029.

Kaganovich D, Kopito R, Frydman J (2008). Misfolded proteins partition between two distinct quality control compartments. Nature 454, 1088–1095.

Kleijnen MF, Roelofs J, Park S, Hathaway NA, Glickman M, King RW, Finley D (2007). Stability of the proteasome can be regulated allosterically through engagement of its proteolytic active sites. Nat Struct Mol Biol 14, 1180–1188.

Kraut DA, Prakash S, Matouschek A (2007). To degrade or release: ubiquitin-chain remodeling. Trends Cell Biol 17, 419–421.

Kriegenburg F, Seeger M, Saeki Y, Tanaka K, Lauridsen AM, Hartmann-Petersen R, Hendil KB (2008). Mammalian 26S proteasomes remain intact during protein degradation. Cell 135, 355–365.

Kulak NA, Pichler G, Paron I, Nagaraj N, Mann M (2014). Minimal, encapsulated proteomic-sample processing applied to copy-number estimation in eukaryotic cells. Nat Methods 11, 319–324.

Laporte D, Lebaudy A, Sahin A, Pinson B, Ceschin J, Daignan-Fornier B, Sagot I (2011). Metabolic status rather than cell cycle signals control quiescence entry and exit. J Cell Biol 192, 949–957.

Laporte D, Salin B, Daignan-Fornier B, Sagot I (2008). Reversible cytoplasmic localization of the proteasome in quiescent yeast cells. J Cell Biol 181, 737–745.

Lee BH, Lu Y, Prado MA, Shi Y, Tian G, Sun S, Elsasser S, Gygi SP, King RW, Finley D (2016). USP14 deubiquitinates proteasome-bound substrates that are ubiquitinated at multiple sites. Nature 532, 398–401.
Li L, Miles S, Breeden LL (2015). A genetic screen for *Saccharomyces cerevisiae* mutants that fail to enter quiescence. G3 (Bethesda) 5, 1783–1795.
Liu CW, Corboy MJ, DeMartino GN, Thomas PJ (2003). Endoproteolytic activity of the proteasome. Science 299, 408–411.
Longtine MS, McKenzie A III, Demarini DJ, Shah NG, Wach A, Brachat A, Philippsen P, Pringle JR (1998). Additional modules for versatile and economical PCR-based gene deletion and modification in *Saccharomyces cerevisiae*. Yeast 14, 953–961.
Marguerat S, Schmidt A, Codlin S, Chen W, Aebersold R, Bahler J (2012). Quantitative analysis of fission yeast transcriptomes and proteomes in proliferating and quiescent cells. Cell 151, 671–683.
Marsh JA, Forman-Kay JD (2010). Sequence determinants of compaction in intrinsically disordered proteins. Biophys J 98, 2383–2390.
Marshall RS, Li F, Gemperline DC, Book AJ, Vierstra RD (2015). Autophagic degradation of the 26S proteasome is mediated by the dual ATG8/ubiquitin receptor RPN10 in *Arabidopsis*. Mol Cell 58, 1053–1066.
Marshall RS, McLoughlin F, Vierstra RD (2016). Autophagic turnover of inactive 26S proteasomes in yeast is directed by the ubiquitin receptor Cue5 and the Hsp42 chaperone. Cell Rep 16, 1717–1732.
Martinez-Munoz GA, Kane P (2008). Vacuolar and plasma membrane proton pumps collaborate to achieve cytosolic pH homeostasis in yeast. Biol J Chem 283, 20309–20319.
McKnight JN, Boerma JW, Breeden LL, Tsukiyama T (2015). Global promoter targeting of a conserved lysine deacetylase for transcriptional shutoff during quiescence entry. Mol Cell 59, 732–743.
Miles S, Li L, Davison J, Breeden LL (2013). Xbp1 directs global repression of budding yeast transcription during the transition to quiescence and is important for the longevity and reversibility of the quiescent state. PLoS Genet 9, e1003854.
Munder MC, Midtvedt D, Franzmann T, Nuske E, Otto O, Herbig M, Ulbricht E, Muller P, Taubenberger A, Maharana S, *et al.* (2016). A pH-driven transition of the cytoplasm from a fluid- to a solid-like state promotes entry into dormancy. eLife 5, e0934710.7554/eLife.09347.
Narayanaswamy R, Levy M, Tsechansky M, Stovall GM, O'Connell JD, Mirrielees J, Ellington AD, Marcotte EM (2009). Widespread reorganization of metabolic enzymes into reversible assemblies upon nutrient starvation. Proc Natl Acad Sci USA 106, 10147–10152.
O'Connell JD, Tsechansky M, Royall A, Boutz DR, Ellington AD, Marcotte EM (2014). A proteomic survey of widespread protein aggregation in yeast. Mol Biosyst 10, 851–861.
O'Farrell PH (2011). Quiescence: early evolutionary origins and universality do not imply uniformity. Philos Trans R Soc Lond B Biol Sci 366, 3498–3507.
Orlowski M, Wilk S (2000). Catalytic activities of the 20 S proteasome, a multicatalytic proteinase complex. Arch Biochem Biophys 383, 1–16.
Parry BR, Surovtsev IV, Cabeen MT, O'Hern CS, Dufresne ER, Jacobs-Wagner C (2014). The bacterial cytoplasm has glass-like properties and is fluidized by metabolic activity. Cell 156, 183–194.
Peters LZ, Hazan R, Breker M, Schuldiner M, Ben-Aroya S (2013). Formation and dissociation of proteasome storage granules are regulated by cytosolic pH. J Cell Biol 201, 663–671.
Peters LZ, Karmon O, David-Kadoch G, Hazan R, Yu T, Glickman MH, Ben-Aroya S (2015). The protein quality control machinery regulates its misassembled proteasome subunits. PLoS Genet 11, e1005178.
Peters LZ, Karmon O, Miodownik S, Ben-Aroya S (2016). Proteasome storage granules are transiently associated with the insoluble protein deposit (IPOD). J Cell Sci 129, 1190–1197 .
Peth A, Uchiki T, Goldberg AL (2010). ATP-dependent steps in the binding of ubiquitin conjugates to the 26S proteasome that commit to degradation. Mol. Cell. 40, 671–681.
Rabl J, Smith DM, Yu Y, Chang SC, Goldberg AL, Cheng Y (2008). Mechanism of gate opening in the 20S proteasome by the proteasomal ATPases. Mol Cell 30, 360–368.
Ratnakumar S, Hesketh A, Gkargkas K, Wilson M, Rash BM, Hayes A, Tunnacliffe A, Oliver SG (2011). Phenomic and transcriptomic analyses reveal that autophagy plays a major role in desiccation tolerance in *Saccharomyces cerevisiae*. Mol Biosyst 7, 139–149.
Rosenzweig R, Bronner V, Zhang D, Fushman D, Glickman MH (2012). Rpn1 and Rpn2 coordinate ubiquitin processing factors at proteasome. J Biol Chem 287, 14659–14671.
Rutledge MT, Russo M, Belton JM, Dekker J, Broach JR (2015). The yeast genome undergoes significant topological reorganization in quiescence. Nucleic Acids Res 43, 8299–313.
Sakata E, Stengel F, Fukunaga K, Zhou M, Saeki Y, Forster F, Baumeister W, Tanaka K, Robinson CV (2011). The catalytic activity of Ubp6 enhances maturation of the proteasomal regulatory particle. Mol Cell 42, 637–649.
Saunier R, Esposito M, Dassa EP, Delahodde A (2013). Integrity of the *Saccharomyces cerevisiae* Rpn11 protein is critical for formation of proteasome storage granules (PSG) and survival in stationary phase. PLoS One 8, e70357.
Shah KH, Nostramo R, Zhang B, Varia SN, Klett BM, Herman PK (2014). Protein kinases are associated with multiple, distinct cytoplasmic granules in quiescent yeast cells. Genetics 198, 1495–1512.
Shimada K, Pasero P, Gasser SM (2002). ORC and the intra-S-phase checkpoint: a threshold regulates Rad53p activation in S phase. Genes Dev 16, 3236–3252.
Tanaka K (2009). The proteasome: overview of structure and functions. Proc Jpn Acad Ser B Phys Biol Sci 85, 12–36.
Tar K, Dange T, Yang C, Yao Y, Bulteau AL, Salcedo EF, Braigen S, Bouillaud F, Finley D, Schmidt M (2014). Proteasomes associated with the Blm10 activator protein antagonize mitochondrial fission through degradation of the fission protein Dnm1. J Biol Chem 289, 12145–12156.
Tong AH, Evangelista M, Parsons AB, Xu H, Bader GD, Page N, Robinson M, Raghibizadeh S, Hogue CW, Bussey H, *et al.* (2001). Systematic genetic analysis with ordered arrays of yeast deletion mutants. Science 294, 2364–2368.
Valcourt JR, Lemons JM, Haley EM, Kojima M, Demuren OO, Coller HA (2012). Staying alive: metabolic adaptations to quiescence. Cell Cycle 11, 1680–1696.
van Deventer S, Menendez-Benito V, van Leeuwen F, Neefjes J (2015). N-terminal acetylation and replicative age affect proteasome localization and cell fitness during aging. J Cell Sci 128, 109–117.
Verma R, Aravind L, Oania R, McDonald WH, Yates JR III, Koonin EV, Deshaies RJ (2002). Role of Rpn11 metalloprotease in deubiquitination and degradation by the 26S proteasome. Science 298, 611–615.
Waite KA, De-La Mota-Peynado A, Vontz G, Roelofs J (2016). Starvation induces proteasome autophagy with different pathways for core and regulatory particles. J Biol Chem 291, 3239–3253.
Wallace EW, Kear-Scott JL, Pilipenko EV, Schwartz MH, Laskowski PR, Rojek AE, Katanski CD, Riback JA, Dion MF, Franks AM, *et al.* (2015). Reversible, specific, active aggregates of endogenous proteins assemble upon heat stress. Cell 162, 1286–1298.
Weberruss MH, Savulescu AF, Jando J, Bissinger T, Harel A, Glickman MH, Enenkel C (2013). Blm10 facilitates nuclear import of proteasome core particles. EMBO J 32, 2697–2707.
Wozniak RW, Rout MP, Aitchison JD (1998). Karyopherins and kissing cousins. Trends Cell Biol 8, 184–188.
Xekardaki A, Kovari E, Gold G, Papadimitropoulou A, Giacobini E, Herrmann F, Giannakopoulos P, Bouras C (2015). Neuropathological changes in aging brain. Adv Exp Med Biol 821, 11–17.
Yao T, Cohen RE (2002). A cryptic protease couples deubiquitination and degradation by the proteasome. Nature 419, 403–407.
Zampar GG, Kummel A, Ewald J, Jol S, Niebel B, Picotti P, Aebersold R, Sauer U, Zamboni N, Heinemann M (2013). Temporal system-level organization of the switch from glycolytic to gluconeogenic operation in yeast. Mol Syst Biol 9, 651.
Zhang J, Vaga S, Chumnanpuen P, Kumar R, Vemuri GN, Aebersold R, Nielsen J (2011). Mapping the interaction of Snf1 with TORC1 in *Saccharomyces cerevisiae*. Mol Syst Biol 7, 545.
Zheng Q, Huang T, Zhang L, Zhou Y, Luo H, Xu H, Wang X (2016). Dysregulation of ubiquitin-proteasome system in neurodegenerative diseases. Front Aging Neurosci 8, 303.
Ziv I, Matiuhin Y, Kirkpatrick DS, Erpapazoglou Z, Leon S, Pantazopoulou M, Kim W, Gygi SP, Haguenauer-Tsapis R, Reis N, *et al.* (2011). A perturbed ubiquitin landscape distinguishes between ubiquitin in trafficking and in proteolysis. Mol Cell Proteomics 10, M111 009753.